

Shape-phase transitions and two-particle transfer intensities

R. Fossion,¹ C. E. Alonso,² J. M. Arias,² L. Fortunato,¹ and A. Vitturi^{1,2}

¹*Dipartimento di Fisica Galileo Galilei and INFN, Via Marzolo 8, I-35131 Padova, Italy*

²*Departamento de Física Atómica, Molecular y Nuclear, Facultad de Física, Universidad de Sevilla, Apartado 1065, E-41080 Sevilla, Spain*

(Received 12 April 2007; published 31 July 2007)

In the light of renewed interest in experiments on two-particle transfer reactions, we study the evolution of the transfer spectroscopic intensities as a possible signature of shape-phase transitions. The study is carried out considering chains of even-even nuclei displaying changes in shape, such as from sphericity to axial-symmetric deformed or from sphericity to deformed γ -unstable nuclei. The evolution of the structure of these nuclei is described in terms of the interacting boson model. In correspondence to the critical points characterizing the phase transitions, the ground-to-ground two-particle transfer matrix elements display a rapid discontinuity, with a corresponding increase in the transition to the excited 0^+ states. Simple formulas are given using the intrinsic-frame formalism.

DOI: [10.1103/PhysRevC.76.014316](https://doi.org/10.1103/PhysRevC.76.014316)

PACS number(s): 21.60.Fw, 21.60.Ev, 21.10.Jx

I. INTRODUCTION

Nucleon-pair-transfer reactions have long since been an important experimental tool for studying nuclear structure. In particular, they have been crucial in obtaining evidence of collective features due to pairing interaction [1,2] or in unraveling the single-particle nature of excited bands in nuclei that feature shape-coexistence phenomena, near to the closed shells, over the entire nuclear chart [3]. Pair-transfer reactions are also useful in the study of nuclear shape-phase transitions, i.e., the rapid evolution of nuclear structure with mass number, such as from sphericity to axial-symmetric deformed or from sphericity to deformed γ -unstable nuclei. Nuclear phase transitions have gained much experimental and theoretical interest recently, after the publication of exact algebraic solutions for excitation spectra and transition rates near the critical points, as, e.g., the so-called E(5) and X(5) solutions [4]. Observables that are often used to follow the evolution of shape transitions are, e.g., ratios of excitation energies such as $R = E_{4_1^+}/E_{2_1^+}$, electromagnetic transitions such as $B(E2; 2_1^+ \rightarrow 0_1^+)$, $B(E0; 0_2^+ \rightarrow 0_1^+)$, and $B(E2; 2_2^+ \rightarrow 0_1^+)/B(E2; 2_2^+ \rightarrow 2_1^+)$, two-neutron separation energies, isomer shifts, and isotope shifts.

In the light of the renewed interest in experiments on pair-transfer reactions [5–8], in the present article we want to investigate how the intensity of the pair-transfer reaction depends on nuclear structure, how the intensity evolves through regions of the nuclear chart where nuclear phase transitions occur, and whether we can specify “fingerprints” in the transfer intensities to locate the critical points of the phase transition. In our study, we will make use of the original version of the interacting boson model, the IBM-1 [9], which describes nuclei by assuming nucleon pairs as basic “building blocks” and treats them as bosons (without making distinction between protons and neutrons). The transfer of one boson to a nucleus thus corresponds to the transfer of a nucleon pair, which makes the IBM model exceptionally well suited to describing two-nucleon transfer reactions.

In a first approach, we will study the intensity of pair transfer in a general way, between ground states, and between ground

state and excited 0^+ states, for phase transitions between the three dynamical limits of the IBM, namely, the U(5) limit (corresponding to a vibrating nucleus), the SU(3) limit (corresponding to an axial-symmetric rotating nucleus), and the O(6) limit (corresponding to a γ -unstable rotating nucleus). In a second step, we will apply our results to some specific series of isotopes, featuring first- and second-order phase transitions. We will compare our results from the IBM with results from the boson coherent-state framework (which can be considered as a mean-field treatment of the IBM), which provides “simple” analytic formulas to describe pair-transfer reactions. We will always consider two-particle transfers in which a particle pair is added to the initial nucleus (stripping reaction). We remind the reader that stripping and pickup reactions have a different selectivity for the population of excited states.

The outline of the present article is as follows. In Sec. II, we first define the pair-transfer operator, and then we summarize the known results from the IBM for the pair-transfer intensities for its three dynamical symmetries: U(5), SU(3), and O(6). In Sec. III, we define, within the boson coherent-state framework, boson condensates for the nuclear ground state 0_1^+ and for the β -vibrational state 0_{bv}^+ , and then derive analytic formulas that describe the intensity of pair-transfer reactions. We check that the results of the IBM and the boson coherent-state framework do agree for the dynamical limits U(5), SU(3), and O(6) in the limit of large N . In Sec. IV, we compare results for pair-transfer intensities from the IBM with results from the boson coherent-state framework in general for transitions between the three dynamical limits of the IBM (Sec. IV A) and for specific series of isotopes that display first- and second-order phase transitions (Sec. IV B). Finally, in Sec. V we present the summary and perspectives.

II. TWO-PARTICLE TRANSFER REACTIONS IN THE IBM

The two-particle transfer process is described by pair creation and annihilation operators that have a straightforward expression within the interacting boson model (IBM).

Of course, this restricts our attention to the transfer of correlated valence bosons (pair of fermions), a situation that is most commonly met in the phenomenology of these kinds of processes leaving aside more complicated transfers involving particles in the core.

Arima and Iachello [9] defined the most general boson equivalent of the $L = 0$ pair-transfer operator $P_{+,0}^{(0)}$, taking into account up to cubic terms, in the form

$$P_{+,0}^{(0)} = p_0 s^\dagger + q_0 [s^\dagger \times s^\dagger]^{(0)} \times \tilde{s}_0^{(0)} + q'_0 [[d^\dagger \times d^\dagger]^{(0)} \times \tilde{s}_0^{(0)}] + q_2 [[d^\dagger \times s^\dagger]^{(2)} \times \tilde{d}_0^{(0)}] + q'_2 [[d^\dagger \times d^\dagger]^{(2)} \times \tilde{d}_0^{(0)}]. \quad (2.1)$$

In the above expression, for specific values of the parameters, some of the terms can be grouped together, and the expression can be recast in the more condensed form

$$P_{+,0}^{(0)} = a_1 s^\dagger + a_2 [\hat{N} \times s^\dagger]^{(0)} + a_3 [\hat{Q} \times d^\dagger]^{(0)}, \quad (2.2)$$

where \hat{Q} is the quadrupole operator,

$$\hat{Q} = (s^\dagger \tilde{d} + d^\dagger s)^{(2)} + \chi (d^\dagger \times \tilde{d})^{(2)}. \quad (2.3)$$

In Eq. (2.2), in analogy with the terminology for atomic absorption and emission of photons, the first term is called the *spontaneous term*. The second term is called the *stimulated term*, in the sense that it contains a factor \hat{N} , which is the number of bosons present. Finally, the third term is called the *quadrupole term*. How to find a satisfactory mapping (from the fermion space to the boson one) to specify the values of the parameters a_i in front of the different terms is not obvious. In the following, we will focus on the spontaneous term, s^+ (or s), which is the leading-order term, while contributions to the transfer intensity from higher order terms will only be briefly discussed in the Appendix. Using the first-order operator, analytic expressions for two-particle transfer intensities I connecting state ϕ in a nucleus with N bosons with state ϕ' in a nucleus with $N + 1$ bosons,

$$I(N, \phi \rightarrow N + 1, \phi') = |\langle [N + 1], \phi' \| s^\dagger \| [N], \phi \rangle|^2, \quad (2.4)$$

have been obtained for the three limits of the IBM: U(5), SU(3), and O(6) [9]. The selection rules for two-particle $L = 0$ transfer in the three limits are summarized in Fig. 2.16 of Ref. [9]. If differences between protons and neutrons are not taken into account (IBM-1), pair-transfer intensities between ground states (gs) of nuclei with N and $N + 1$ bosons read [9]

$$I_{\text{gs-gs}}^{\text{U}(5)} = N + 1, \quad (2.5)$$

$$I_{\text{gs-gs}}^{\text{SU}(3)} = \frac{N + 2}{3} + \frac{1}{3(2N + 1)}, \quad (2.6)$$

$$I_{\text{gs-gs}}^{\text{O}(6)} = \frac{N + 3}{2} - \frac{1}{N + 2}. \quad (2.7)$$

In the U(5) case, transitions to all other 0^+ states vanish. In the SU(3) and O(6) cases, one obtains the following values for the transitions between the ground state (gs) of a nucleus with N bosons and the β -vibrational state (bv) of a nucleus with

$N + 1$ bosons [9],

$$I_{\text{gs-bv}}^{\text{SU}(3)} = \frac{2}{3} + \frac{2}{3(4N^2 - 1)}, \quad (2.8)$$

$$I_{\text{gs-bv}}^{\text{O}(6)} = \frac{1}{2} - \frac{1}{(N + 1)(N + 2)}, \quad (2.9)$$

whereas in all limits the transfer intensity to the double- β and higher phonon excited states vanishes. It is worth noting that within this paper, we will use the term “ β vibration” (bv) to indicate the bandhead of the “quasi- β ” excitation, namely, the bandhead of the β -rotational band in the SU(3) case ($\lambda = 2N - 4, \mu = 2$ band), and the bandhead of the β -vibrational band in the O(6) case ($\sigma = N - 2, v = 0$ band). Similarly we will use the term “double- β vibration” for the bandheads ($\lambda = 2N - 8, \mu = 4$) and ($\sigma = N - 4, v = 0$) in the two cases.

In the three limits, for large values of N , the intensity becomes linearly increasing in N for one pair transfer between two ground states, it approaches a constant value for a transfer between the ground state and the β -vibrational state, and it finally vanishes for the double- β state (dbv). Note that the transfers to excited states are therefore in the three limits either null or orders of magnitude weaker than the ground-state transfer. Outside the three dynamical limits, calculations have to be done numerically, and no closed analytical expressions are obtained.

III. TWO-PARTICLE TRANSFER REACTIONS IN THE BOSON COHERENT-STATE FRAMEWORK

A. Boson coherent-state framework

Whenever a theory is formulated in terms of quantum variables, one faces the problem of interpreting it in terms of geometrical variables. This has been accomplished for the interacting boson model with the introduction of boson coherent intrinsic states that provide a bridge between the U(6) algebraic formulation and the Bohr-Mottelson model (which can be thought of as the five-dimensional coset space of the IBM, labeled by five coordinates that can be put in correspondence with the α_μ of the collective description) [10–12]. Recent insight into the relationship between the dynamical symmetries of the IBM and the collective model may be found in Ref. [13].

Intrinsic states allow the evaluation of expectation values of operators that can be associated with observables and have been successfully used to compare theoretical predictions with experimental data. The matrix elements of the pair-transfer operators can thus be effectively treated in this formalism, which allows one to not only study the magnitude and relevance of the transfer probability as a function of shape variables, but also follow the behavior of this observable across a shape-phase transition or along a chain of neighbor isotopes. Within the intrinsic-state framework, it is possible to perform calculations in the large- N limit, where numerical calculations in the IBM are not possible.

In the intrinsic-frame formalism, the ground state of a nucleus with N bosons can be expressed as a boson condensate with specific quadrupole deformation parameters β and γ [9].

Using the operator b_{gs}^\dagger , defined as

$$b_{\text{gs}}^\dagger(\beta, \gamma) = \frac{1}{\sqrt{1+\beta^2}} \left(s^\dagger + \beta \cos \gamma d_0^\dagger + \frac{\beta}{\sqrt{2}} \sin \gamma (d_2^\dagger + d_{-2}^\dagger) \right), \quad (3.1)$$

we get for the ground state,

$$\begin{aligned} |N; \text{gs}(\beta, \gamma)\rangle &= \frac{1}{\sqrt{N!}} (b_{\text{gs}}^\dagger(\beta, \gamma))^N |0\rangle \\ &= \frac{1}{\sqrt{N!}} \frac{1}{(1+\beta^2)^{N/2}} \left(s^\dagger + \beta \cos \gamma d_0^\dagger \right. \\ &\quad \left. + \frac{\beta}{\sqrt{2}} \sin \gamma (d_2^\dagger + d_{-2}^\dagger) \right)^N |0\rangle. \end{aligned} \quad (3.2)$$

Also intrinsic excitations can be described within the coherent-state framework by replacing one of the bosons in the condensate by an orthogonal combination of the s^\dagger and d^\dagger operators. We define the b_{bv}^\dagger operator as

$$b_{\text{bv}}^\dagger(\beta, \gamma) = \frac{1}{\sqrt{1+\beta^2}} \left(-\beta s^\dagger + \cos \gamma d_0^\dagger + \frac{1}{\sqrt{2}} \sin \gamma (d_2^\dagger + d_{-2}^\dagger) \right), \quad (3.3)$$

and we get for the β -vibrational state,

$$\begin{aligned} |N; \text{bv}(\beta, \gamma)\rangle &= \frac{1}{\sqrt{N}} b_{\text{bv}}^\dagger(\beta, \gamma) b_{\text{gs}}^\dagger(\beta, \gamma) |N; \text{gs}(\beta, \gamma)\rangle \\ &= \frac{1}{\sqrt{(N-1)!}} \frac{1}{(1+\beta^2)^{N/2}} \\ &\quad \times \left(-\beta s^\dagger + \cos \gamma d_0^\dagger + \frac{1}{\sqrt{2}} \sin \gamma (d_2^\dagger + d_{-2}^\dagger) \right) \\ &\quad \times \left(s^\dagger + \beta \cos \gamma d_0^\dagger \right. \\ &\quad \left. + \frac{\beta}{\sqrt{2}} \sin \gamma (d_2^\dagger + d_{-2}^\dagger) \right)^{N-1} |0\rangle. \end{aligned} \quad (3.4)$$

In a similar way, the replacement of other bosons in the condensate with additional orthogonal combinations of s^\dagger and d^\dagger operators gives rise to the intrinsic states associated with double- β vibrations and to higher order vibrations. We know that the use of the intrinsic states allows one to reproduce, in leading order in $1/N$, the exact excitation energies and multipole transitions. As we will see in the next section, this will also be the case for the transfer matrix elements.

B. Two-particle transfer reactions in the boson coherent-state framework

The effect of the s^\dagger operator on the pair transfer between two ground states $|N; \text{gs}(\beta, \gamma)\rangle \rightarrow |N+1; \text{gs}(\beta', \gamma')\rangle$ [see Eq. (3.2)] and between a ground state and a β -vibrational state $|N; \text{gs}(\beta, \gamma)\rangle \rightarrow |N+1; \text{bv}(\beta', \gamma')\rangle$ [see Eqs. (3.2) and (3.4)]

can be evaluated by using the boson commutator relations [14]

$$\begin{aligned} [b_i, f(b)] &= \frac{\partial}{\partial b_i^\dagger} f(b), \\ [f(b), b_i^\dagger] &= \frac{\partial}{\partial b_i} f(b), \end{aligned} \quad (3.5)$$

$f(b)$ being a polynomial in $b_1^\dagger, b_2^\dagger, \dots$, and b_1, b_2, \dots . We obtain for the matrix element between the ground states of a nucleus with N bosons and a nucleus with $N+1$ bosons, with quadrupole deformations β, γ and β', γ' ,

$$\begin{aligned} \langle N+1; \text{gs}(\beta', \gamma') || s^\dagger || N; \text{gs}(\beta, \gamma) \rangle \\ = \sqrt{N+1} \frac{[1 + \beta\beta' \cos(\gamma - \gamma')]^N}{\sqrt{(1+\beta'^2)^{N+1}(1+\beta^2)^N}}. \end{aligned} \quad (3.6)$$

Similarly, we can obtain the expression for the matrix element of the pair transfer s^\dagger between the ground state of a nucleus with N bosons and the bandhead of the β -vibrational band of a nucleus with $N+1$ bosons, with respective quadrupole deformations β, γ and β', γ' , respectively,

$$\begin{aligned} \langle N+1; \text{bv}(\beta', \gamma') || s^\dagger || N; \text{gs}(\beta, \gamma) \rangle \\ = \frac{[1 + \beta\beta' \cos(\gamma - \gamma')]^{N-1}}{\sqrt{(1+\beta'^2)^{N+1}(1+\beta^2)^N}} (N[\beta \cos(\gamma - \gamma') \\ - \beta'] - \beta'[1 + \beta\beta' \cos(\gamma - \gamma')]), \end{aligned} \quad (3.7)$$

and for the transition to the double- β -vibrational state,

$$\begin{aligned} \langle N+1; \text{dbv}(\beta', \gamma') || s^\dagger || N; \text{gs}(\beta, \gamma) \rangle \\ = \sqrt{\frac{N}{2}} [\beta \cos(\gamma - \gamma') - \beta'] \frac{[1 + \beta\beta' \cos(\gamma - \gamma')]^{N-2}}{\sqrt{(1+\beta'^2)^{N+1}(1+\beta^2)^N}} \\ \times ((N-1)[\beta \cos(\gamma - \gamma') - \beta'] \\ - 2\beta'[1 + \beta\beta' \cos(\gamma - \gamma')]). \end{aligned} \quad (3.8)$$

The above expressions allow us to calculate pair-transfer intensities between nuclei with N and $N+1$ nucleons, using as input information only the quadrupole deformations β, γ and β', γ' of the two nuclei. This input can be obtained from experimental or theoretical mass compilations, as long as the proper conversion between the different definitions of β is taken into account.

For the three dynamical IBM limits, the predictions from the boson coherent-state formalism should correspond in leading order to those from the IBM (in the limit $N \rightarrow \infty$). Within the boson coherent-state formalism, we obtain the pair-transfer intensities assuming as quadrupole deformations $\beta = \beta' = 0$ for U(5). For SU(3), we will take the parameters associated with the minima in the energy surfaces for large N , i.e., $\beta = \beta' = \sqrt{2}$ and $\gamma = \gamma' = 0$. In the O(6) limit, where the energy surface is γ independent, we will take $\beta = \beta' = 1$, and an averaged value for γ which coincides for both the nuclei with N and $N+1$ bosons. We obtain, for ground-state to

ground-state transfer, the formulas

$$\mathcal{I}_{\text{gs-gs}}^{\text{U}(5)}(\beta = \beta' = 0) = (N + 1), \quad (3.9)$$

$$\mathcal{I}_{\text{gs-gs}}^{\text{SU}(3)}(\beta = \beta' = \sqrt{2}) = \frac{(N + 1)}{3}, \quad (3.10)$$

$$\mathcal{I}_{\text{gs-gs}}^{\text{O}(6)}(\beta = \beta' = 1) = \frac{(N + 1)}{2}. \quad (3.11)$$

For the transition between the ground state and the β -vibrational state, we get

$$\mathcal{I}_{\text{gs-bv}}^{\text{U}(5)}(\beta = \beta' = 0) = 0, \quad (3.12)$$

$$\mathcal{I}_{\text{gs-bv}}^{\text{SU}(3)}(\beta = \beta' = \sqrt{2}) = \frac{2}{3}, \quad (3.13)$$

$$\mathcal{I}_{\text{gs-bv}}^{\text{O}(6)}(\beta = \beta' = 1) = \frac{1}{2}, \quad (3.14)$$

while the intensity for transfer to higher phonon excited states vanishes in the three limits [because of the factor $(\beta - \beta')$ in Eq. (3.8), and likewise factors for higher phonon states]. In the case of the $\text{gs} \rightarrow \text{bv}$ pair-transfer reaction, it can be seen immediately that the intensity predictions for the three limits within the boson coherent-state framework agree with the predictions from the IBM, which saturate quickly to a constant value for large N ; similarly for the double- β vibrations, where we obtain the correct asymptotically vanishing value. In the case of a $\text{gs} \rightarrow \text{gs}$ transfer, for the U(5) limit, both models predict precisely the same transfer probability (linear in N). For the SU(3) and O(6) limits, however, for large N , the IBM predictions are somewhat larger than the predictions within the boson coherent-state framework by a constant term, which is $1/3$ in the SU(3) limit and 1 in the O(6) limit. The ratio between both predictions, however, goes asymptotically to unity, as shown in in Fig. 1, and we can conclude that the predictions from both models correspond for large values of N for all three dynamical limits, U(5), SU(3), and O(6).

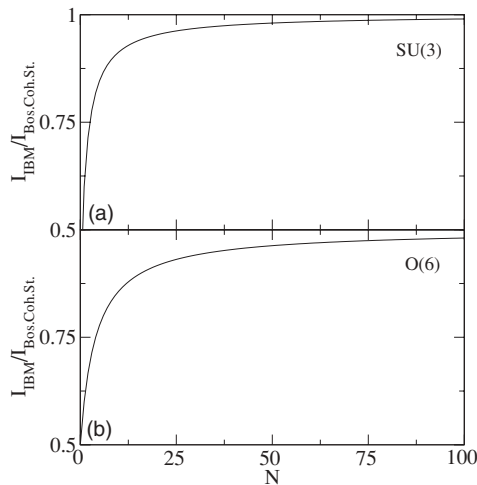


FIG. 1. Ratios of the IBM and boson coherent-state predictions for the pair-transfer intensity, for the SU(3) and O(6) limits. For both limits and for large N , the ratio between the two predictions goes to unity.

IV. FINGERPRINTS OF NUCLEAR PHASE TRANSITIONS IN PAIR-TRANSFER REACTIONS, COMPARISON BETWEEN IBM AND BOSON COHERENT-STATE RESULTS

In this section, we want to find fingerprints of nuclear phase transitions in the intensity of pair-transfer reactions. First, as described in Sec. IV A, we study the evolution of the pair-transfer intensity as one moves between two vertices of the IBM symmetry triangle, and compare predictions from the IBM and the boson coherent-state formalism. Second, in Sec. IV B, we study some real isotope series that are known to perform phase transitions of first and second order (the ${}_{60}\text{Nd}$, ${}_{62}\text{Sm}$, ${}_{64}\text{Gd}$ and ${}_{66}\text{Nd}$ isotope series, and the ${}_{44}\text{Ru}$ isotope series, respectively), and we make predictions of how the intensity of pair-transfer reactions evolve, especially close to the critical point. Finally, we suggest fingerprints, of particular interest to experimentalists, to pin down the critical point of the phase transition.

A. Application to the IBM symmetry triangle

The construction of potential energy surfaces (PESs) is a powerful and very visual tool, often used in mean-field studies, to see how nuclear structure and nuclear binding energies evolve over large regions of nuclei. PESs have also been used in mean-field studies to analyze the critical points in series of isotopes that perform nuclear phase transitions [15,16]. In the IBM, starting from the boson coherent-state approach, β -constrained PESs have been constructed, and their evolution, when moving between the different dynamic limits, have been studied thoroughly [9,14]. We can use the absolute minima, β_{min} , of PESs, describing nuclei with N and $N + 1$ bosons, as input in the “simple” formulas in the boson coherent-state framework, Eqs. (3.6) and (3.7), to calculate transfer intensities. In the present section, we want to study how the pair-transfer intensity evolves when we cross the IBM symmetry triangle between two of its symmetry limits, i.e., from U(5) to O(6), from U(5) to SU(3), and from O(6) to SU(3). To proceed, we adopt the usual model Hamiltonian that describes the way the IBM symmetry triangle will be covered, that is,

$$\hat{H} = (1 - \xi)\hat{n}_d - \frac{\xi}{N}\hat{Q}(\chi) \cdot \hat{Q}(\chi), \quad (4.1)$$

with the quadrupole operator $\hat{Q}(\chi)$ given by Eq. (2.3). We get the PES by calculating the expectation value of this transitional Hamiltonian on the boson condensate [Eq. (3.2)], again using the boson commutator relations of Eq. (3.5),

$$E(\beta) = (1 - \xi) \left(N \frac{\beta^2}{1 + \beta^2} \right) - \xi \left[\frac{1}{1 + \beta^2} (5 + (1 + \chi^2)\beta^2) + \frac{N - 1}{(1 + \beta^2)^2} \left(\frac{2}{7}\chi^2\beta^4 - 4\sqrt{\frac{2}{7}}\chi\beta^3 \cos 3\gamma + 4\beta^2 \right) \right]. \quad (4.2)$$

For $\xi = 0$, we get the U(5) limit; for $\xi = 1$ and $\chi = 0$, the O(6) limit; and for $\xi = 1$ and $\chi = -\frac{\sqrt{7}}{2}$, the SU(3) limit. For

intermediate values of the control parameters ξ and χ , the PES function will describe a certain point on the IBM symmetry triangle, located between the three limits. To describe a phase transition, one has to establish the value of the control parameter for each nucleus. As a consequence, one has to determine the functional relations $\xi = \xi(N)$ and/or $\chi = \chi(N)$. In the study of a real series of nuclei, the latter functionals of course need to be determined from experimental data. One can, however, propose a simple function to obtain some physical insight into the structure of the pair-transfer intensity. In the following, to fix the idea, we consider a series of isotopes with a number of bosons that can vary between $N = 5$ and $N = 15$. To describe the $U(5) \rightarrow O(6)$ transition, the parameter χ was chosen as 0. In the transition $U(5) \rightarrow SU(3)$, χ was fixed at $-\sqrt{7}/2$. In both cases, the transition is obtained by varying the value of the parameter ξ . For this, different functional dependencies can be used, as, e.g., a linear or a quadratic one [17]. These parametrizations were chosen because they allow a consistent description of global nuclear properties (as, e.g., binding energies) together with local nuclear properties (nuclear structure, nuclear deformation, etc.), through a long series of nuclei, as a function of the mass number A . In the following, however, we will prefer a Fermi dependence, because it stresses the ‘‘abruptness’’ of the critical point. The different parametrizations, linear, quadratic, and Fermi, respectively, are

$$\xi = 0.1N - 0.5, \quad (4.3)$$

$$\xi = 0.005N^2 - 0.125, \quad (4.4)$$

$$\xi = \frac{1}{1 + \exp\left(\frac{N_0 - N}{\Delta}\right)}. \quad (4.5)$$

Using the linear and quadratic parametrizations (4.3) and (4.4), ξ ranges from 0 to 1 for N going from 5 to 15. In the Fermi parametrization (4.5), N_0 symbolizes the nucleus where the phase transition is supposed to happen, and Δ is the extent over which the phase transition is ‘‘smeared out.’’ In the following, we will take the example of $N_0 = 9$ and $\Delta = 0.5$ to model a rather fast phase transition.

1. From spherical to γ -unstable [$U(5)$ to $O(6)$ transition]

In the following, we adopt the Fermi function, Eq. (4.5). The $U(5)$ - $O(6)$ transition is obtained by choosing $\chi = 0$ in the transitional Hamiltonian. The system goes from $U(5)$ to $O(6)$ when the number of bosons is increasing from $N = 5$ toward $N = 15$ (and therefore ξ is increasing from 0 to 1). Results for the $U(5)$ to $O(6)$ phase transition are given in Fig. 2. The PESs are independent in γ and are given in panel (a), as a function of β for boson numbers $N = 5$ –15. The minima, $\beta_{\min}(N)$, of these surfaces are represented in panel (b) and used as input for the formulas for the matrix elements of the transfer-reaction intensity, Eqs. (3.6) and (3.7), in the boson coherent-state framework. For γ and γ' , we take again an averaged value that coincides for both the nuclei with N and $N + 1$ bosons. Finally, we compare results for the transfer intensities from the IBM model and the boson coherent-state

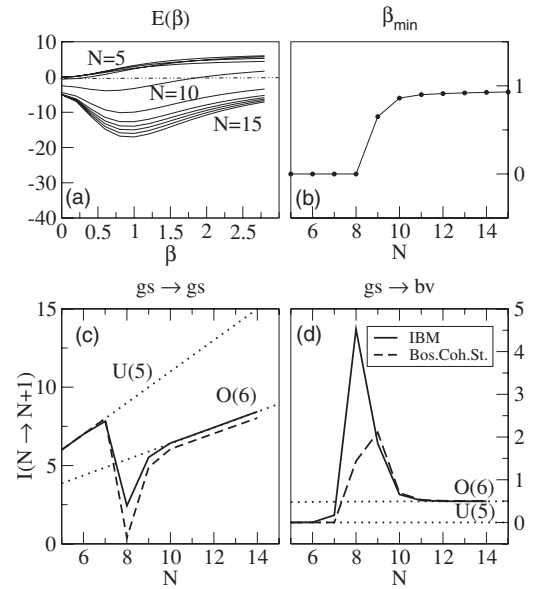


FIG. 2. From spherical to γ unstable, $U(5)$ - $O(6)$. (a) Cuts of PESs for $N = 5$ –15 in function of the quadrupole deformation β , and (b) position of the absolute minima β_{\min} of the different PESs. Two-particle transfer intensities calculated in the IBM (solid lines) and the boson coherent-state framework (dashed lines) are shown in (c) for the $gs \rightarrow gs$ transfer and in (d) for the $gs \rightarrow bv$ transfer. The IBM predictions for the $U(5)$ and $O(6)$ limits are also indicated (dotted lines).

framework for a ground-state to ground-state transfer [panel (c)], and for transfer between the ground state and the β -vibrational state [panel (d)]. It can be seen in the figure that in both the IBM and the boson coherent-state calculations, for the $gs \rightarrow gs$ and $gs \rightarrow bv$ transfers, the intensities are close to the predictions of the $U(5)$ limit for small N , while approaching the $O(6)$ limit for large N , through a softer (IBM) or more abrupt (boson coherent-state framework) phase transition with a sudden change in the intensity at $N = 8$. In the case of the boson coherent-state approach, the abruptness in the intensities is caused by the discontinuity in the β_{\min} values at $N = 9$. As we study transfers $I(N \rightarrow N + 1)$, the jump in the intensities appears already for $N = 8$. In general, within both models, the intensity for a transfer between two ground states [panel (c)] is larger than the intensity for a transfer toward the β -vibrational state [panel (d)]. At the critical point, however, the transfer to the ground state loses strength, whereas the transfer to the β -vibrational state gains strength. In the specific case represented in Fig. 2, the boson coherent-state formulas predict larger values for the intensities with respect to the transfer to the ground state. As already remarked in Sec. III, for $gs \rightarrow gs$ transfers, for large N , the IBM and boson coherent-state results for the $O(6)$ limit differ by a constant term; this is why in panel (c) it appears as if the IBM and boson coherent-state results would not coincide. We have pointed out, however, that the ratio between both goes asymptotically toward unity, so that both models are equivalent in the large N limit.

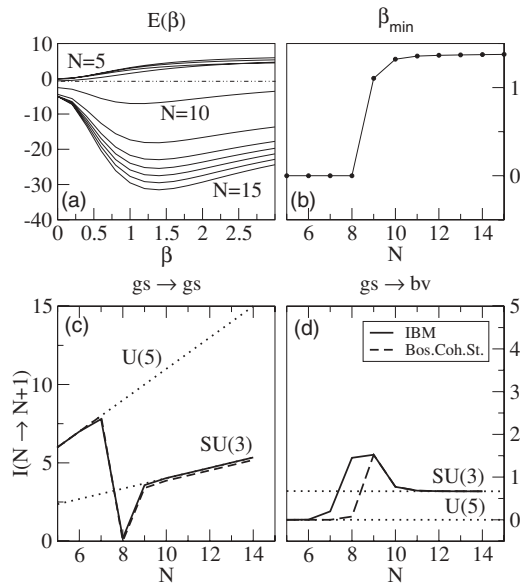


FIG. 3. From spherical to axial-symmetric deformed, U(5)-SU(3). (a) Cuts of PESs for $N = 5-15$ and for $\gamma = \gamma' = 0$ in function of the quadrupole deformation β , and (b) position of the absolute minima β_{\min} of the different PESs. Two-particle transfer intensities calculated in the IBM (solid lines) and the boson coherent-state framework (dashed lines) are shown in (c) for the $gs \rightarrow gs$ transfer and in (d) for the $gs \rightarrow bv$ transfer. The IBM predictions for the U(5) and SU(3) limits are also indicated (dotted lines).

2. From spherical to axial-symmetric deformed [U(5) to SU(3) transition]

As in the preceding case, we adopt here a Fermi dependence for the control parameter ξ , while χ is kept fixed at the value $\chi = -\frac{\sqrt{7}}{2}$. The system passes from the U(5) to the SU(3) limit when the number of bosons is increasing from $N = 5$ toward $N = 15$ (or alternatively when ξ is increasing from 0 to 1). Results are displayed in Fig. 3. In panel (a), the PESs [see Eq. (4.2)] are given for boson numbers from $N = 5$ to $N = 15$. The minima, $\beta_{\min}(N)$, of these surfaces are represented in panel (b), and are again used as input for the formulas providing the matrix elements for the transfer reaction, Eqs. (3.6) and (3.7), in the boson coherent-state framework. In panel (c), results for the transfer intensities from the IBM model and the boson coherent-state framework are compared for ground-state to ground-state transfer, and in panel (d) for transfer between ground state and β -vibrational state. In general, within both models, the intensity for a transfer between two ground states [panel (c)] is larger than the transfer to the β -vibrational state [panel (d)]. At the critical point, however, the transfer to the ground state loses strength, whereas the transfer to the β -vibrational state gains strength. In the specific case shown in Fig. 3, at the critical point, both models even predict larger values for the intensities with respect to the transfer to the ground state. Again, it should be noted that the IBM and the boson coherent-state calculations, for the SU(3) limit, for the $gs \rightarrow gs$ transition, differ by a constant term $1/3$, which is the reason that in panel (c) the IBM and the boson

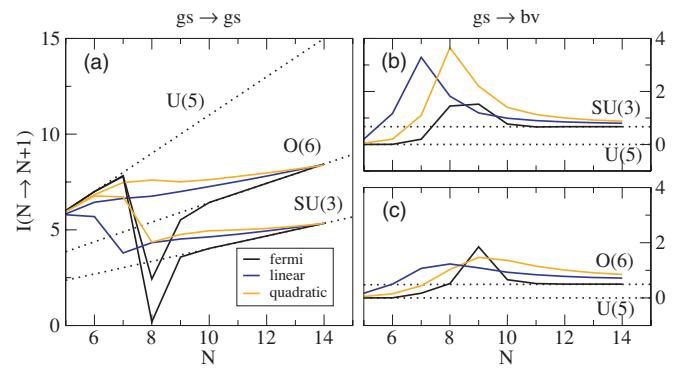


FIG. 4. (Color online) Dependence of two-particle transfer intensities on the phase-transition path (Fermi, linear, and quadratic functions are shown), for (a) a $gs \rightarrow gs$ transfer for U(5)-O(6) and U(5)-SU(3), and for a $gs \rightarrow bv$ transfer for (b) U(5)-SU(3) and (c) U(5)-O(6). The IBM predictions for the U(5), O(6), and the SU(3) limits are also indicated (dotted lines).

coherent-state results do not exactly coincide for the largest N presented.

3. Effects of the choice of the phase-transitional path

In our general theoretical study, we need to specify the functional form $\xi(N)$ that governs the way in which the nuclei change structure through the phase-transitional region. In Fig. 4, the effect of choosing different phase-transitional paths [linear, quadratic, or Fermi $\xi(N)$] is shown [Eqs. (4.3), (4.4), and (4.5), respectively] in the case of the IBM calculation, for $gs \rightarrow gs$ transfer [panel (a)], and for $gs \rightarrow bv$ transfer [panels (b) and (c)]. One can note that, although the specific position of the critical point of the phase transition depends on the chosen transitional path, and the abruptness of the phase transition can vary, in general the evolutions of the transfer intensities are qualitatively very similar.

4. From γ -unstable to axial-symmetric deformed (O(6) to SU(3) cross-over)

Besides the two phase transitions considered previously, one can also inquire into the nuclear structure along the “deformed leg” of the IBM symmetry triangle. This corresponds to a transition path from the O(6) to the SU(3) limit. This can be described, for example, using a single quadrupole-quadrupole Hamiltonian, varying the parameter χ in the quadrupole operator between the limiting values 0 [O(6)] and $-\sqrt{7}/2$ [SU(3)]. For an explicit functional dependence on the particle number N , we suggest again a Fermi phase-transitional path,

$$\chi(N) = \frac{-\sqrt{7}/2}{1 + \exp\left(\frac{N_0 - N}{\Delta}\right)}, \quad (4.6)$$

where $\Delta = 0.5$, $N_0 = 9$, and N runs from 5 to 15. Using the β_{\min} of the resulting PESs as input for the formulas (3.6) and (3.7) in the boson coherent-state framework, we present in Fig. 5 the results for the transfer intensities for $gs \rightarrow gs$ transfers [panel (a)] and $gs \rightarrow bv$ transfers [panel (b)], and

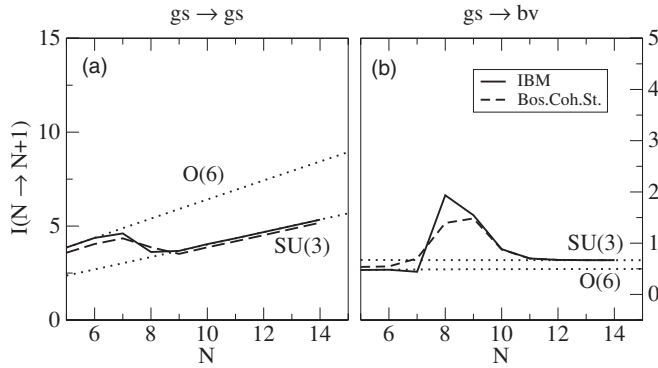


FIG. 5. From γ -unstable to axial-symmetric deformed, O(6)-SU(3). Predictions from the IBM model (solid lines) and from the boson coherent-state framework (dashed lines) for $gs \rightarrow gs$ and $gs \rightarrow bv$ transfers. The IBM predictions for the O(6) and SU(3) limits are also indicated (dotted lines).

we compare them with numerical calculations from the IBM. As we study transfers $I(N \rightarrow N + 1)$, the discontinuity in the β_{\min} at $N_0 = 9$ shows up already in the intensities at $N = 8$. For the $gs \rightarrow gs$ transfer, the transition between the two limits is very smooth in the case of the IBM, and even smoother in the case of the boson coherent-state framework. This is perfectly consistent with the fact that in this case the path is not associated with a phase transition, but with a so-called cross-over. For the $gs \rightarrow bv$ transfer [panel (b)], however, the IBM (and to a lesser degree the boson coherent-state framework) produces a “bump” in the intensities of approximately the same magnitude as in the U(5) to SU(3) or U(5) to O(6) transitions. To clarify this point, we show in Fig. 6 the population of the different 0^+ states along the transition paths U(5)-O(6) (top) and U(5)-SU(3) (middle) and the cross-over O(6)-SU(3) (bottom). The figure clearly shows a large fragmentation of the transfer strength at the critical and cross-over points. In the case of the cross-over, this fragmentation is probably responsible for the local enhancement of the $gs \rightarrow bv$ transfer intensity. Such

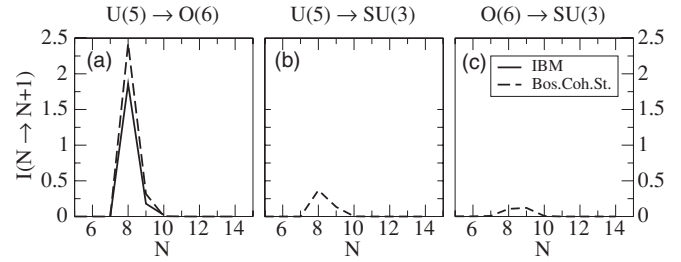


FIG. 7. Intensities for $gs \rightarrow dbv$ pair transfer, within the boson coherent-state framework (dashed lines), for the U(5)-O(6) and U(5)-SU(3) transitions and the O(6)-SU(3) cross-over. For the U(5)-O(6) transition, the IBM prediction is also given (solid line).

a fragmentation should be observed in two-particle stripping experiments.

5. Transfer to double- β -vibrational states

Clear discontinuities at the critical points are also evidenced by the pair-transfer intensities to higher excited 0^+ states. In Fig. 7, we show the intensities for the transitions to the double- β -vibrational states. In the U(5)-O(6) and U(5)-SU(3) transitions [panels (a) and (b)], using the Fermi transition path in Eq. (4.5), with $N_0 = 9$, $\Delta = 0.5$, and $N = 5-15$, the intrinsic-frame approach shows [and the IBM calculations confirm for the U(5)-O(6) transition] that a sudden strong peak appears in the transfer intensity in correspondence to the critical point. A similar behavior can also be expected for the transition to higher excited states. Because of the large fragmentation for the U(5)-SU(3) transition and the O(6)-SU(3) cross-over, already discussed in relation to Fig. 6, it was impossible to single out the double- β -vibrational state close to the critical and cross-over points. In our specific case of the O(6)-SU(3) cross-over [panel (c)], using the Fermi transition path in Eq. (4.6) with $N_0 = 9$, $\Delta = 0.5$, and $N = 5-15$, the transfer intensity at the critical point is nonzero, but very small.

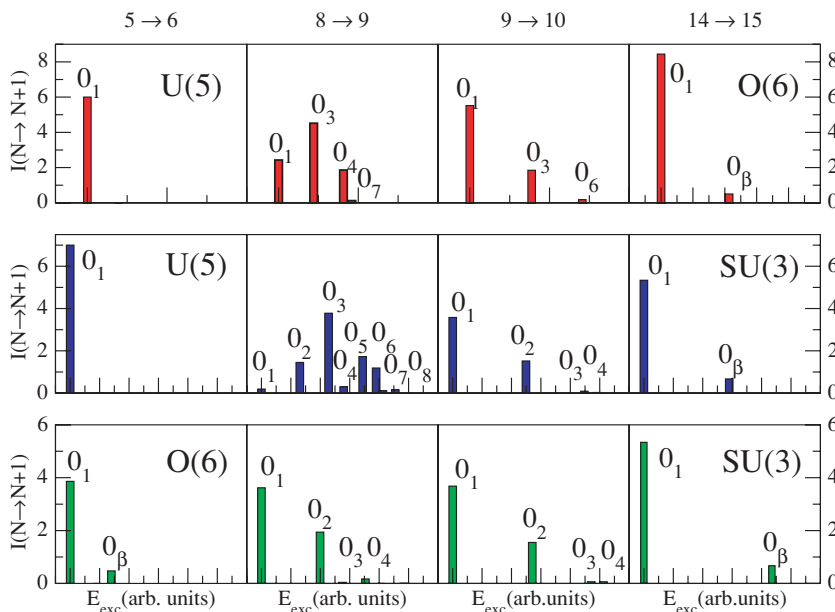


FIG. 6. (Color online) Fragmentation of the two-particle transfer intensity for the U(5)-O(6) transition (top row), the U(5)-SU(3) transition (middle row), and the U(5)-SU(3) cross-over (bottom row). Whereas near the dynamic limits U(5), O(6), and SU(3) for $N = 5 \rightarrow 6$ and $14 \rightarrow 15$, transfer only occurs between ground states or the β -vibrational excited 0^+_{β} , near the critical or cross-over point $N = 9$, the transfer intensity is fragmented over a large number of excited 0^+ states, and it is not obvious as to how to identify the β -vibrational or double- β -vibrational state.

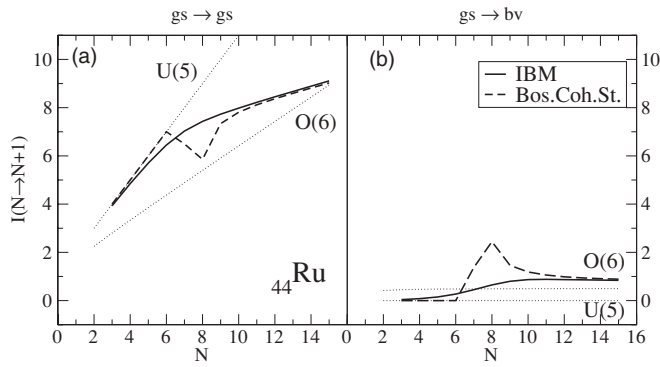


FIG. 8. Two-particle transfer intensities for the $^{94-118}\text{Ru}$ isotopes vs total boson number N (with $N = N_\pi + N_\nu$, and number of proton bosons $N_\pi = 3$, and number of neutron bosons $N_\nu = 0-12$), for the $\text{gs} \rightarrow \text{gs}$ and $\text{gs} \rightarrow \text{bv}$ transfers.

One is led to conclude that the appreciable excitation of excited 0^+ states in transfer processes, in correspondence with a loss of intensity in the transfer to the ground state, can be assumed as a signature of the occurrence of a shape transition.

B. Application to some real isotope chains

Applications to real series of isotopes are presented in Fig. 8 for a second-order phase transition $\text{U}(5) \rightarrow \text{O}(6)$ (Ru isotope series), and in Fig. 9 for a first-order phase transition $\text{U}(5) \rightarrow \text{SU}(3)$ (Nd, Sm, Gd, and Dy isotope series).

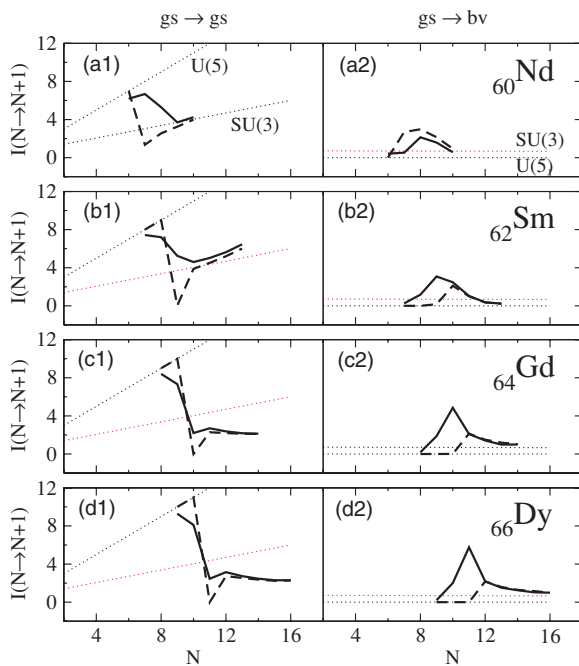


FIG. 9. (Color online) Two-particle transfer intensities for the $^{144-154}\text{Nd}$ (with $N_\pi = 5$ proton bosons and $N_\nu = 1-6$ neutron bosons), $^{146-160}\text{Sm}$ ($N_\pi = 6$ and $N_\nu = 1-8$), $^{148-162}\text{Gd}$ ($N_\pi = 7$ and $N_\nu = 1-8$), and $^{150-166}\text{Dy}$ ($N_\pi = 8$ and $N_\nu = 1-9$) isotope chains vs the total number of bosons N (with $N = N_\pi + N_\nu$), for the $\text{gs} \rightarrow \text{gs}$ and $\text{gs} \rightarrow \text{bv}$ transfers.

1. $\text{U}(5)$ to $\text{O}(6)$ transition: Ru isotopes

The Ru isotopes display a transitional behavior from spherical $[\text{U}(5)]$ to γ -unstable $[\text{O}(6)]$ shapes (second-order phase transition) [18,19]. A systematic study of the Ru isotopes was carried out by a simultaneous least-squares fit to the energies of these nuclei in Refs. [18,19]. The Hamiltonian used is

$$H = \epsilon \hat{n}_d + \kappa_0 \hat{P}^\dagger \hat{P} + \kappa_1 \hat{L} \cdot \hat{L} + \kappa_3 \hat{T}_3 \cdot \hat{T}_3 - \frac{\kappa_0}{4} N(N+4), \quad (4.7)$$

with the different operators defined by

$$\hat{n}_d = \sum_{\mu} d_{\mu}^{\dagger} d_{\mu}, \quad (4.8)$$

$$\hat{P}^{\dagger} = \frac{1}{2} (d^{\dagger} \cdot d^{\dagger} - s^{\dagger} s^{\dagger}), \quad (4.9)$$

$$\hat{L} = \sqrt{10} (d^{\dagger} \times \tilde{d})^{(1)}, \quad (4.10)$$

$$\hat{T}_3 = (d^{\dagger} \times \tilde{d})^{(3)}. \quad (4.11)$$

A fit of the low-lying states in the whole isotope chain provides the following values for the parameters (all in keV): $\epsilon = 887 - 53N$, $\kappa_0 = 93.2$, $\kappa_1 = 11.66$, and $\kappa_3 = 61.6$. The parameters are kept fixed for all the isotopes; the only variation in going from one isotope to the other is the change in ϵ induced by the variation in the boson number N . The boson number was obtained considering closed shells at 50 for both neutrons and protons. In Ref. [19] the energy surfaces were calculated and the isotope with $N = 8$ (^{104}Ru) was identified as critical. In this work, we used this parametrization without any parameter tuning as a realistic example of realization of a second-order phase-transition from $\text{U}(5)$ to $\text{O}(6)$ and calculated two-neutron transfer intensities along the Ru isotope chain. As mentioned before, we used as pair-transfer operator just the leading term s^{\dagger} . In Fig. 8, the pair-transfer intensity is plotted vs boson number, transfer is done from isotope N to $N + 1$. Dotted lines give the $\text{U}(5)$ and $\text{O}(6)$ limiting values. Both transfers from ground-to-ground [panel (a)] and from ground-to-quasi- β bands [panel (b)] are plotted. Full lines give the exact IBM calculation obtained with the parameters given above, while dashed lines give the results produced by the boson coherent-state framework (the latter results are strictly valid only in large N limit). Light isotopes are close to the vibrational $\text{U}(5)$ limit, while heavy isotopes are closer to the $\text{O}(6)$ limit, as expected. For N around 8 (transfer from $N = 7$ to $N = 8$ and from $N = 8$ to $N = 9$), a drop down is observed in the ground-to-ground pair-transfer intensity at the mean-field level, reflecting that the structures of the isotopes involved are changing rapidly. A complementary increase in the ground-to-quasi- β pair-transfer intensity at the mean-field level is also observed. In the actual IBM calculation, the effect of finite N smears out this change in a wider region around $N = 8$.

2. $\text{U}(5)$ to $\text{SU}(3)$ transition: Rare-earth isotopes

As an illustration of a first-order phase transitions, we present calculations of pair-transfer intensities for the isotope chains ^{60}Nd , ^{62}Sm , ^{64}Gd , and ^{66}Dy . In this region, nuclear

shapes evolve from spherical to axial-symmetric deformed. In Ref. [20], a systematic study of isotope chains in the rare-earth region including $^{144-154}_{60}\text{Nd}$, $^{146-160}_{62}\text{Sm}$, $^{148-162}_{64}\text{Gd}$, and $^{150-166}_{66}\text{Dy}$ isotope chains was presented. The most general (up to two-body terms) IBM Hamiltonian was used, and for each isotope chain a general fit was performed in such a way that all parameters but one were kept fixed to describe the whole chain.

Such a general IBM Hamiltonian, in multipolar form, can be written as

$$\hat{H} = \varepsilon_d \hat{n}_d + \kappa_0 \hat{P}^\dagger \hat{P} + \kappa_1 \hat{L} \cdot \hat{L} + \kappa_2 \hat{Q} \cdot \hat{Q} + \kappa_3 \hat{T}_3 \cdot \hat{T}_3 + \kappa_4 \hat{T}_4 \cdot \hat{T}_4, \quad (4.12)$$

where the quadrupole operator \hat{Q} is given by Eq. (2.3) (here used with $\chi = -\frac{\sqrt{7}}{2}$), the operators \hat{n}_d , \hat{P}^\dagger , \hat{L} , and \hat{T}_3 were defined in Eqs. (4.8)–(4.11), and

$$\hat{T}_4 = (d^\dagger \times \tilde{d})^{(4)}. \quad (4.13)$$

The parameters used in Hamiltonian (4.12) can be found in Ref. [20]. We used these parameters without any additional tuning. In Ref. [20], the energy surfaces were calculated and the catastrophe theory was used to determine critical points for each isotope chain. For all these chains, the shapes of the light isotopes are close to sphericity, while the shapes of the heavy ones are close to axial deformations. This transition is known to be of first order. We have calculated pair-transfer intensities with the operator s^\dagger , as in the preceding case. In Fig. 9, the pair-transfer intensity from isotope N to $N + 1$ is plotted vs the neutron number. Dot-dashed lines give the U(5) and SU(3) limiting values. Again, both transfer intensities from ground-to-ground and from ground-to-quasi- β bandheads are plotted. Solid lines give the exact IBM calculation obtained with the parameters given above, while dashed lines give the results produced by the boson coherent-state framework (mean field). In all the isotope chains studied, a drop down is observed in ground-to-ground pair-transfer intensities at the mean-field level for a given value of N , reflecting that the structures of the isotopes involved are changing rapidly. A complementary increase in the ground-to-quasi- β pair-transfer intensity at the mean-field level is also observed. In the actual IBM calculation, the effect of finite N seems to be not so important as in the Ru case. Abrupt drops in ground-to-ground transfer intensity with the complementary increments in the ground-to- β intensities clearly mark the phase transition in the case of the Nd, Sm, Gd, and Dy isotope series.

V. CONCLUSIONS

The study of nuclear phase transitions has always been a topic of interest, but it has attracted more attention since the recent publication of exact algebraic solutions for nuclear excitation spectra and electromagnetic transitions near the critical points, such as E(5) and X(5) [4]. There are many experimental observables that can be used to follow the evolution of nuclear phase transitions through long series of isotopes. One of them is the intensity of nucleon-pair transfer, which we have studied in the present paper, with particular

attention to its behavior close to the critical points. We carried out our study within the interacting boson model (IBM-1). In particular, we studied the transfer between ground states, between the ground state and the β -vibrational 0^+ excited state, and between the ground state and higher phonon excited 0^+ states. We compared IBM results with results from the boson coherent-state framework. In the latter model, we were able to derive “simple” algebraic formulas that only need as input the quadrupole deformation β and β' of the nuclei between which the pair transfer takes place.

We first carried out our study in a general way between each of the three dynamic limits of the IBM symmetry triangle: U(5), O(6), and SU(3). Next, we applied our results to some specific series of isotopes that are known to display phase transitions of first and second order (the ^{60}Nd , ^{62}Sm , ^{64}Gd and ^{66}Dy series, and the ^{44}Ru series, respectively). In conclusion, the intensity for pair transfer between two ground states is in general much larger than the intensity for transfer between the ground state and the β -vibrational or higher phonon 0^+ excited states. At the critical point, however, for U(5) to O(6) and U(5) to SU(3) (second-order and first-order transitions, respectively) both the IBM and the boson coherent-state framework predict sudden changes in the evolution of the transfer intensity: the $\text{gs} \rightarrow \text{gs}$ transfer loses in strength, whereas the intensity for $\text{gs} \rightarrow \text{bv}$ and $\text{gs} \rightarrow \text{dbv}$ transfer show a peak. This feature is especially present in the first-order phase transition, where in some cases the population of the ground states becomes even smaller than those to the β vibrational 0^+ . Such a “flip” is shown in Fig. 3 for the theoretical study of the U(5)-SU(3) transition for $N = 5-15$ bosons, and in Fig. 9 in panels (c) and (d) for the Gd and Dy isotope series. No inversion of the $\text{gs} \rightarrow \text{gs}$ and $\text{gs} \rightarrow \text{bv}$ transfer intensities is observed for the Nd and Sm isotopes, panels (a) and (b) of Fig. 9. Also for the O(6)-SU(3) cross-over, we predict a jump in the intensity for the $\text{gs} \rightarrow \text{bv}$ pair transfer, which is smaller but of the same order of magnitude as the corresponding bumps in the case of the U(5)-O(6) and U(5)-SU(3) transitions. As it is well known, no phase transition is present in the O(6)-SU(3) cross-over, although we observe sudden changes in the transfer intensities, which are due to the increased density of states and mixing of wave functions. The $\text{gs} \rightarrow \text{dbv}$ intensity, however, is very small for the O(6) to SU(3) cross-over. One is tempted to conclude that the appreciable excitation of excited 0^+ states in transfer processes, in correspondence with a loss of intensity in the transfer to the ground state, can be assumed to be a signature of the occurrence of a shape transition.

ACKNOWLEDGMENTS

The authors want to thank K. Heyde and F. Iachello for valuable theoretical remarks, and P. Van Duppen for the experimental interest that stimulated the present theoretical work. This work has been partially supported by the Spanish Ministerio de Educación y Ciencia and by the European Regional Development Fund (FEDER) under Project No. FIS2005-01105, and by INFN. Andrea Vitturi acknowledges financial support from SEUI (Spanish Ministerio de Educación y Ciencia) for a sabbatical year at the University of Seville.

APPENDIX

We have defined the boson equivalent of the pair-transfer operator in Eq. (2.2) and worked out the formulas (3.6), (3.7), and (3.8) for the transfer intensity within the boson coherent-state framework, using the lowest order term s^\dagger for the $gs \rightarrow gs$, $gs \rightarrow bv$, and $gs \rightarrow dbv$ transfers, respectively. The higher order terms $[\hat{N} \times s^\dagger]^{(0)}$ and $[\hat{Q} \times d^\dagger]^{(0)}$ in the boson equivalent of the pair-transfer operator can be worked out in an analog way. For axial symmetry, we obtain for a $gs \rightarrow gs$ and $gs \rightarrow bv$ transfer,

$$\begin{aligned} & \langle N+1; gs(\beta') | [\hat{N} \times s^\dagger]^{(0)} | N; gs(\beta) \rangle \\ &= N \sqrt{N+1} \frac{(1+\beta\beta')^N}{\sqrt{(1+\beta^2)^{N+1}(1+\beta^2)^N}}, \\ & \langle N+1; gs(\beta') | [\hat{Q} \times d^\dagger]^{(0)} | N; gs(\beta) \rangle \\ &= N \sqrt{N+1} \frac{(1+\beta\beta')^{N-1}}{\sqrt{(1+\beta^2)^{N+1}(1+\beta^2)^N}} \\ & \quad \times (\chi\beta\beta^2 + \beta^2 + \beta\beta'), \end{aligned}$$

and for a $gs \rightarrow bv$ transfer,

$$\begin{aligned} & \langle N+1; bv(\beta') | [\hat{N} \times s^\dagger]^{(0)} | N; gs(\beta) \rangle \\ &= N \frac{(1+\beta\beta')^{N-1}}{\sqrt{(1+\beta^2)^{N+1}(1+\beta^2)^N}} \\ & \quad \times [-\beta'(1+\beta\beta') + N(\beta - \beta')], \\ & \langle N+1; bv(\beta') | [\hat{Q} \times d^\dagger]^{(0)} | N; gs(\beta) \rangle \\ &= N \frac{(1+\beta\beta')^{N-2}}{\sqrt{(1+\beta^2)^{N+1}(1+\beta^2)^N}} \\ & \quad \times [-(1+\beta\beta')(-2\beta' - \beta + \beta\beta^2 - 2\chi\beta\beta') \\ & \quad + (N-1)\beta\beta'(2 + \chi\beta')(\beta - \beta')]. \end{aligned}$$

As already pointed out earlier, how to find a satisfactory mapping to specify the parameters a_i in front of the different terms is not obvious. A careful comparison between theoretical predictions and experimental data might shed light on the ratios a_i/a_j ($i, j = 1, 2, 3$) between the different parameters.

-
- [1] R. A. Broglia, O. Hansen, and C. Riedel, in *Adv. in Nucl. Phys.*, edited by M. Baranger and E. Vogt (Plenum Press, New York, 1973), Vol. 6, p. 287.
- [2] W. von Oertzen and A. Vitturi, *Rep. Prog. Phys.* **64**, 1247 (2001).
- [3] K. Heyde *et al.*, *Phys. Rep.* **102**, 291 (1983); J. L. Wood *et al.*, *ibid.* **215**, 101 (1992).
- [4] F. Iachello, *Phys. Rev. Lett.* **85**, 3580 (2000); F. Iachello, *Phys. Rev. Lett.* **87**, 052502 (2001).
- [5] D. Bucurescu *et al.*, *Phys. Rev. C* **73**, 064309 (2006).
- [6] D. A. Meyer *et al.*, *Phys. Rev. C* **74**, 044309 (2006).
- [7] D. A. Meyer *et al.*, *Phys. Lett.* **B638**, 44 (2006).
- [8] P. Van Duppen *et al.*, ISOLDE Collaboration, CERN, internal communication.
- [9] F. Iachello and A. Arima, *The Interacting Boson Model* (Cambridge University Press, Cambridge, 1987).
- [10] J. N. Ginocchio and M. W. Kirson, *Phys. Rev. Lett.* **44**, 1744 (1980).
- [11] A. E. L. Dieperink, O. Scholten, and F. Iachello, *Phys. Rev. Lett.* **44**, 1747 (1980).
- [12] A. Bohr and B. R. Mottelson, *Phys. Scr.* **22**, 461 (1980).
- [13] D. J. Rowe and G. Thiamova, *Nucl. Phys.* **A760**, 59 (2005).
- [14] P. Van Isacker and J.-Q. Chen, *Phys. Rev. C* **24**, 684 (1981).
- [15] R. Fossion, D. Bonatsos, and G. A. Lalazissis, *Phys. Rev. C* **73**, 044310 (2006).
- [16] Z.-Q. Sheng and J.-Y. Guo, *Mod. Phys. Lett. A* **20**, 2711 (2005).
- [17] J. E. García-Ramos, C. De Coster, R. Fossion, and K. Heyde, *Nucl. Phys.* **A688**, 735 (2001).
- [18] A. Frank, P. Van Isacker, and D. D. Warner, *Phys. Lett.* **B197**, 474 (1987).
- [19] A. Frank, C. E. Alonso, and J. M. Arias, *Phys. Rev. C* **65**, 014301 (2001).
- [20] J. E. García-Ramos, J. M. Arias, J. Barea, and A. Frank, *Phys. Rev. C* **68**, 024307 (2003).